# Anisotropic 3D Amplitude Variation with Azimuth (AVAZ) Methods to Detect Fracture Prone Zones in Tight Gas Resource Plays

Bill Goodway*
EnCana Corp., Calgary, AB, Canada
william.goodway@encana.com

and

John Varsek and Christian Abaco
EnCana Corp., Calgary, AB, Canada

## 3D Seismic AVAZ Ambiguities

AVAZ interpretation for fracture attributes can be established by models using theory based on HTI anisotropy (horizontal transverse isotropy). However comparing figures 6 and 7 show opposing predictions for both the orientation and intensity of anisotropy with no single and obvious guiding principle. The Williams and Jenner model (fig.6), is compelling as it logically explains the expected weaker 3D stack response to fractures. This is due to a decreasing (negative) gradient perpendicular to fractures, while the isotropic or parallel case has a flat gradient and hence a strong stack response in areas where no fractures exist. By contrast industry's AVAZ model prediction shown in figure 7, is exactly opposed as the relative stack response would be stronger perpendicular to fractures than the isotropic or fracture parallel equivalent. It is interesting to note that this lack of generality is unlike the isotropic AVO type gradient classification (Rutherford and Williams 1989) that is diagnostic of changes in Vp/Vs ratio.

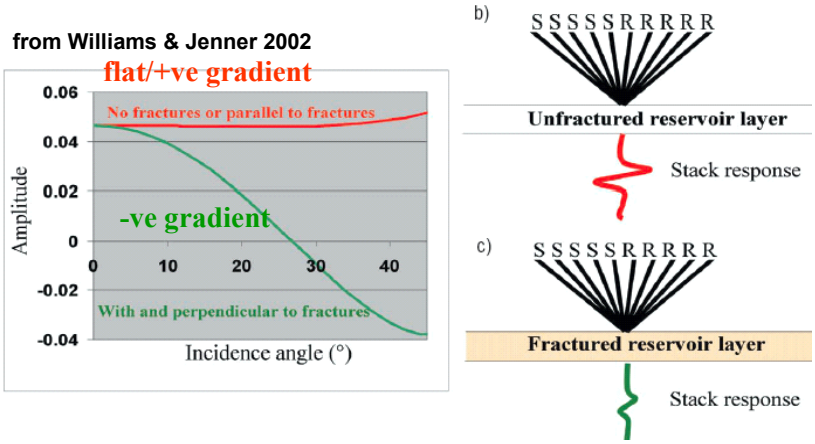


**Figure 6.** AVAZ variation with stack response:
- parallel is strong (flat to +ve gradient)
- perpendicular is weak (-ve gradient)

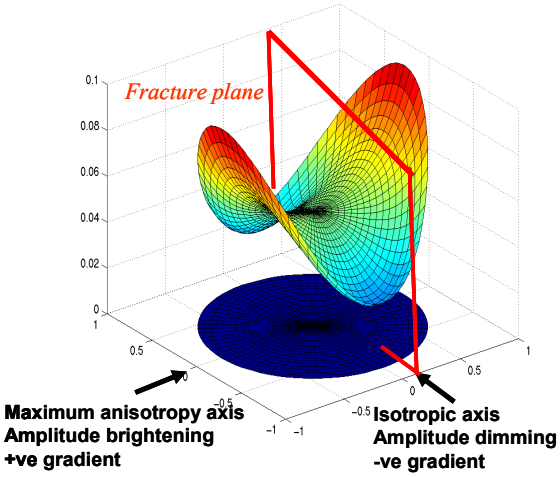


**Figure 7.** Amplitude variation in HTI medium as advertised by contractor industry. (polar azimuth plots of gradients modelled from Ruger's AVAZ equation)

A better understanding of these ambiguities requires some investigation into the theory primarily developed by Ruger (Ruger and Tsvankin 1997). Figure 8 shows the azimuthal AVO gradient variation for two models with different anisotropic parameters from Ruger's TLE paper, that are based on his equation and from which the following observations can be drawn:

1) the magnitude of the gradient variation with azimuth is much smaller than the basic isotropic AVO gradient despite a realistic choice of values for anisotropic parameters between 8% and 15%

2) the magnitude of gradient variation with azimuth shown by model examples in figures 6 and 7, are significantly larger than those predicted by Ruger's equation even to the point of reversing the sign of the gradient (compare figures 7 and 8)

3) the relative stack response from a fractured vs. isotropic layer can be consistent or at odds with one's intuition (compare figures 6, 7 and 8)

4) the zero offset reflection has no azimuth variation.

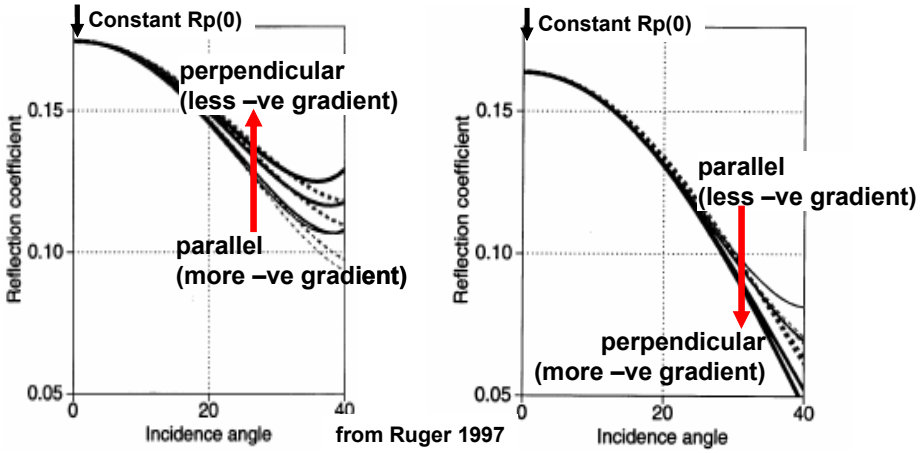


**Figure 8.** Ruger's models based on his linearized 3 term azimuthal AVO gradient equation.

## Anisotropic AVO Theory and Models from Ruger's equation

Inversion for P-wave anisotropy follows from isotropic AVO by utilizing Ruger's anisotropic reformulation of the Aki and Richards linearized equation for P-wave reflectivity with incidence angle (Aki and Richards 1980) and is based on a simple HTI model of vertically aligned fractures as shown in figure 9.

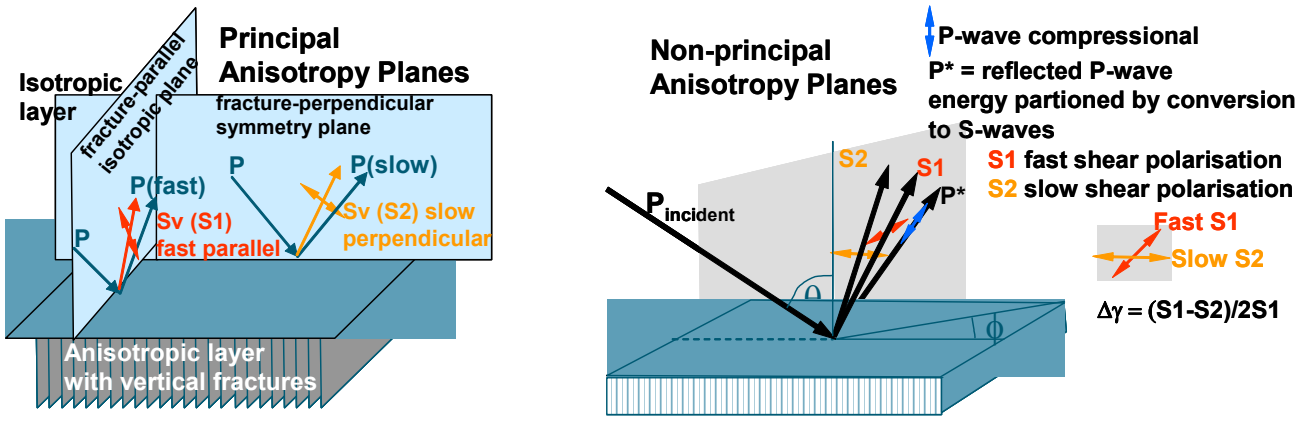


**Figure 9.** Model of HTI media used in Ruger's 1997 AVAZ P-wave reflection equation showing anisotropic conversion to shear-waves for principal and non-principal planes of symmetry.

The HTI model is identical in its transverse isotropy (TI) to the more familiar vertical transverse isotropy (VTI) model for horizontal layers e.g. shales. However for the HTI model both $\varepsilon$ and $\delta$ (VTI case) undergo a transformation to $\varepsilon^{(v)}$ and $\delta^{(v)}$ where (v) denotes a vertical axis reference due to the 90° symmetry axis rotation from their VTI equivalents as given in equation 3.

$$\varepsilon^{(v)} = -\frac{\varepsilon}{1+2\varepsilon} \qquad \delta^{(v)} = \frac{\delta - 2\varepsilon}{1+2\varepsilon}\frac{f+\varepsilon}{f+2\varepsilon} \qquad \text{where } f = 1 - \frac{\beta_0^2}{\alpha_0^2} \qquad \text{(eqn.3)}$$

and for completeness (as used in equation 5)

$$\Rightarrow \varepsilon^{(v)} - \delta^{(v)} = \frac{-\left[(\delta - 2\varepsilon) + \varepsilon\right](f + 2\varepsilon)}{(1+2\varepsilon)(f+2\varepsilon)} + \frac{(\delta - 2\varepsilon)\varepsilon}{f+2\varepsilon} \approx \frac{\varepsilon - \delta}{1+2\varepsilon} \quad (\text{ignoring } (\delta - 2\varepsilon)\varepsilon << 1)$$

$$\varepsilon^{(v)} - \delta^{(v)} = \frac{\varepsilon - \delta}{1+2\varepsilon} = \eta^* \cong \eta \quad \text{following} \quad \eta = \frac{\varepsilon - \delta}{1+2\delta} \quad (\text{Alkhalifa and Tsvankin 1995})$$

Consequently these HTI parameters $\varepsilon^{(v)}$ and $\delta^{(v)}$ along with the VTI $\gamma$, appear in Ruger's HTI AVAZ reflection equation for azimuth angles $\phi$ between the principal symmetry axis plane and isotropic plane as shown in equation 4.

$$Rp(\theta,\phi) = A + (B_{iso} + B_{aniso})\sin^2\theta + (C_{iso} + C_{aniso})\tan^2\theta\sin^2\theta \qquad \text{(eqn. 4)}$$

where:

$$A = 0.5\frac{\Delta\alpha_0}{\alpha_0} + 0.5\frac{\Delta\rho}{\rho} = Rp(0)$$

$$B_{iso} = 0.5\left[\frac{\Delta\alpha_0}{\alpha_0} - \left(\frac{2\beta_0}{\alpha_0}\right)^2\frac{\Delta\mu}{\mu}\right] \qquad B_{aniso} = 0.5\left[\Delta\delta^{(v)} + 2\left(\frac{2\beta_0}{\alpha_0}\right)^2\Delta\gamma\right]\cos^2\phi$$

$$C_{iso} = 0.5\frac{\Delta\alpha_0}{\alpha_0} \qquad C_{aniso} = 0.5\left[\Delta\delta^{(v)}\sin^2\phi\cos^2\phi + \Delta\varepsilon^{(v)}\cos^4\phi\right]$$

Incidence angle $\theta$, $\alpha_0$ and $\beta_0$ are averaged across reflection interface between HTI and overlying layer

HTI Thomsen parameters $\Delta\gamma, \Delta\varepsilon^{(v)}$ and $\Delta\delta^{(v)}$ are differences in anisotropy from HTI to overlying layer

$\phi$ = azimuth angle with respect to symmetery axis plane where $\phi = 0$

For the isotropic plane, equation 4 follows from the Aki and Richards equation and is based on vertical fractional contrasts or reflectivity in density $\Delta\rho/\rho$ P-wave velocity $\Delta\alpha/\alpha$ and rigidity $\Delta\mu/\mu$ (Wang 1999, Goodway 2000). However Ruger chose the approach of Shuey (Shuey 1985) by gathering the $\Delta\alpha/\alpha$, $\Delta\varepsilon^{(v)}$ and $\Delta\delta^{(v)}$ terms with significant contrast ($C_{iso}$ $C_{aniso}$), into the third higher order incidence angle $\sin^2\theta$ $\tan^2\theta$ term. The consequence of this is similar to the isotropic case where both AVO and AVAZ equations do not have the critical curvature discrimination at high incidence angle when used in industry practice as two term approximations (see figures 10a and 10b). However the relative contribution of the 2nd vs. 3rd term is far worse of a problem in the AVAZ case. This leads to fundamental ambiguities and hence errors involved in azimuthal anisotropy inversion. It also explains the wide variation and confusion in observation or interpretation of AVAZ effects in data and model examples shown above and in the literature (Goodway 2006).

Using values established from logs in the case study area, figures 10a and 10b, show the AVAZ curve variation with incidence angle from parallel (isotropic plane) to perpendicular (symmetry axis plane) for a two layer isotropic/HTI model, comparing the two term (A and $B\sin^2\theta$) Shuey type approximation as used in practice, to the full three term Ruger equation 4.

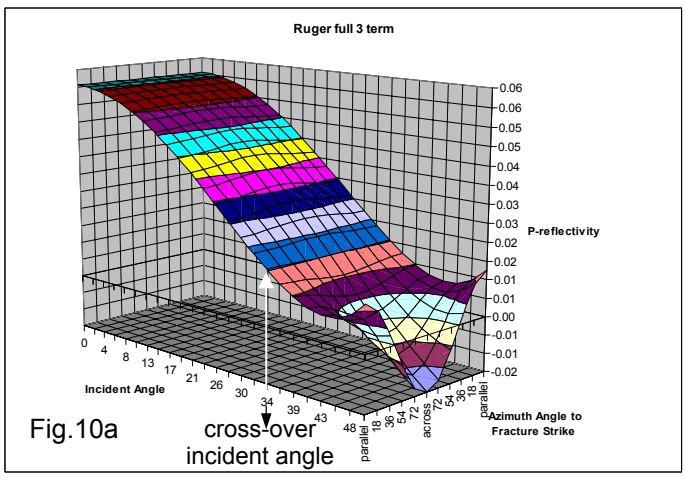


Fig.10a cross-over incident angle

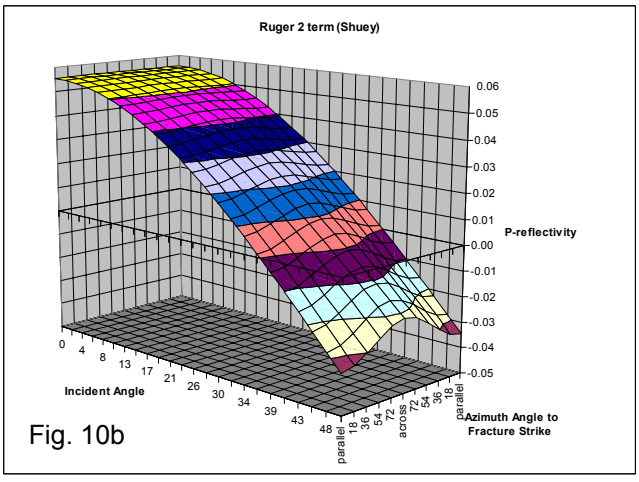


Fig. 10b

**Figure 10.** 10a and 10b: 3D displays of Ruger's 3 term vs. 2 term (Shuey) equation of azimuthal AVO curves.

The following observations can be drawn:

1) The full 3 term curves are similar to those shown by Ruger for gas filled fractures with similar HTI parameters $\gamma$ = 0.085, $\varepsilon^{v}$ =-0.15 and $\delta^{v}$ = -0.155, (figure 8 above) where very little separation can be seen between the curves for varying azimuth for incidence angles up to 35º. However at reasonably large angle ranges between 35º to 45º, discrimination between azimuths is possible due to the curvature in the 3 term equation. The curvature diminishes with decreasing azimuth angle $\phi$ from parallel to fractures (isotropic plane) to perpendicular or across fractures (symmetry axis plane)

2) The two term approximation used in practice shows a large and opposed separation in azimuth AVO curves for most of the incidence angle range from 20º to 45º and is unable to match the critically diagnostic 3 term curvature beyond 35º

3) The most startling observations are that using a 2 term Shuey approximation to fit the actual 3 term measurement would produce a result that showed no azimuthal anisotropy for angles less than 35º and the wrong opposed 90º fracture azimuth for angles greater than 35º !

The reason for these observations is that the 2nd term in Ruger's equation is reduced in significance below $\theta$ = 35º incidence angle, as a result of the $B_{aniso}$ term having anisotropic parameters $\gamma$ and $\delta^{(v)}$ with opposing sign (see equation 3). Consequently the 3rd high incidence angle term ($C_{iso}C_{aniso}$ in equation 4) has more impact on the azimuthal gradient and cannot be ignored. In fact in a yet more ambiguous way a "cross-over" angle occurs at 33.9º where for $\theta$ < 33.9º the "parallel to fractures" (isotropic) azimuth AVO curve is below that of the "perpendicular to fractures" (symmetry axis plane) curve and reverses this sense for $\theta$ > 33.9º with a greater, more visible separation (see figure 10a).

Given the importance of the 3rd term in Ruger's equation, a better approach would be to rewrite the equation in three terms of equal significance. The result shown in equations 5 and 6, has a zero incidence angle term in $\Delta\alpha/\alpha$ and two isotropic/anisotropic terms in $\sin^2\theta$ (with $\Delta\mu/\mu$) and $\tan^2\theta$ (with $\Delta\alpha/\alpha$). For the elliptical gas filled fracture case the underlying physical connection of the impact of the HTI anisotropic parameters $\Delta\varepsilon^{(v)}$ (-ve sign) and $\Delta\gamma$ (+ve sign) can be seen as respectively reducing the isotropic AVO gradient terms for $\Delta\alpha/\alpha$ and $\Delta\mu/\mu$ as these are the parameters associated with the P-wave phase velocity and shear-wave splitting due to fractures (see equation 6).

$$Rp(\theta,\phi) = 0.5\frac{\Delta\rho}{\rho} + 0.5\frac{\Delta\alpha}{\alpha} + 0.5\left[\frac{\Delta\alpha}{\alpha} + \left\{\Delta\delta^{(v)} + \left(\Delta\varepsilon^{(v)} - \Delta\delta^{(v)}\right)\cos^2\phi\right\}\cos^2\phi\right]\tan^2\theta$$

$$-0.5\left[\left(\frac{2\beta}{\alpha}\right)^2\frac{\Delta\mu}{\mu} - \left\{2\left(\frac{2\beta}{\alpha}\right)^2\Delta\gamma - \left(\Delta\varepsilon^{(v)} - \Delta\delta^{(v)}\right)\cos^2\phi\right\}\cos^2\phi\right]\sin^2\theta \qquad \text{(eqn.5)}$$

and with the following substitution based on equation 3

$$\Delta\varepsilon^{(v)} - \Delta\delta^{(v)} \approx \frac{\Delta\varepsilon - \Delta\delta}{1+2\varepsilon} = \eta^* \text{ obtainable from NMO through } \eta = \frac{\Delta\varepsilon - \Delta\delta}{1+2\delta} \text{ (Alkhalifah and Tsvankin 1995)}$$

$$\Rightarrow Rp(\theta,\phi) = 0.5\frac{\Delta\rho}{\rho} + 0.5\frac{\Delta\alpha}{\alpha} + 0.5\left[\frac{\Delta\alpha}{\alpha} + \left\{\Delta\delta^{(v)} + \eta^*\cos^2\phi\right\}\cos^2\phi\right]\tan^2\theta$$

$$-0.5\left[\left(\frac{2\beta}{\alpha}\right)^2\frac{\Delta\mu}{\mu} - \left\{2\left(\frac{2\beta}{\alpha}\right)^2\Delta\gamma - \eta^*\cos^2\phi\right\}\cos^2\phi\right]\sin^2\theta$$

Next by dropping the first small constant $\frac{\Delta\rho}{\rho}$ term

and for elliptical anisotropy (the gas filled fracture case under consideration) $\Delta\delta^{(v)} = \Delta\varepsilon^{(v)}$

$$\Rightarrow Rp(\theta,\phi) = 0.5\frac{\Delta\alpha}{\alpha} + 0.5\left[\frac{\Delta\alpha}{\alpha} + \Delta\varepsilon^{(v)}\cos^2\phi\right]\tan^2\theta + 0.5\left(\frac{2\beta}{\alpha}\right)^2\left[2\Delta\gamma\cos^2\phi - \frac{\Delta\mu}{\mu}\right]\sin^2\theta \qquad \text{(eqn.6)}$$

A relatively robust 3 term method for inversion of azimuthal anisotropic parameters based on equation 6 would exploit the separation between the 2nd term's $\tan^2\theta\cos^2\phi$ surface and the 3rd term's $\sin^2\theta\cos^2\phi$ surfaces shown in figures 11a and 11b.

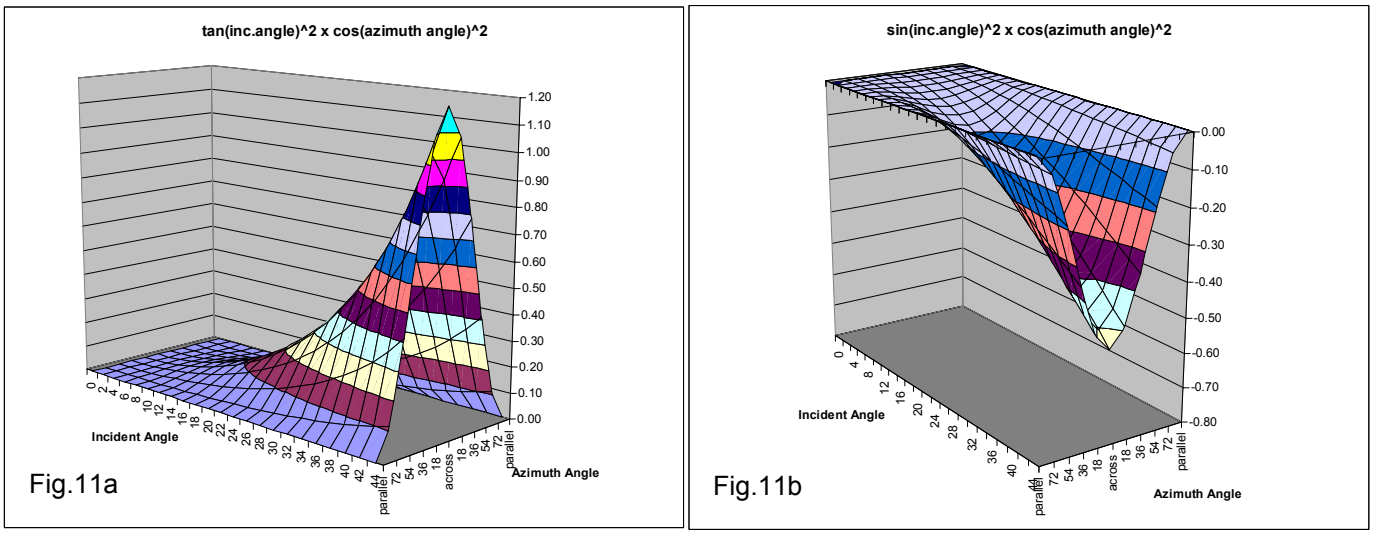


**Figure 11.** 11a and 11b; 3D displays of new 3 term AVAZ equation 6: 11a is the 2nd term and 11b is the 3rd term

## Conclusions

Seismic 3D AVAZ used to detect anisotropy due to fractures or stress, offers the only opportunity to directly identify fracture prone zones prior to committing to significant horizontal well drilling costs. This paper describes the anisotropic AVAZ method that can be applied to map and predict optimal drilling locations. Beyond describing standard industry AVAZ practice, some fundamental theoretical and practical ambiguities of the method to correctly detect the orientation and intensity of anisotropy are revealed. Through an understanding of these ambiguities, constraints can be placed on the method as demonstrated by 3D case studies from the WCSB and a new approach and set of equations are developed that improve the ability of the technology to establish the presence of fracture prone zones and hence optimum gas recovery.

**References**


Aki K., and Richards P.G., 1980, Quantitative Seismology, W.H.Freeman & Co.

Grigg M., 2004 Gas Shale Technology Exchange, SPE.

Goodway W., 2001 “AVO and Lamé constants for rock parameterization and fluid detection” June CSEG Recorder

Goodway W. Varsek J. and Abaco C., 2006 “Practical applications of P-wave AVO for unconventional gas Resource Plays-2 Detection of fracture prone zones with Azimuthal AVO and coherence discontinuity” CSEG Recorder April 2006

Ruger, A., and Tsvankin, I., 1997 “Using AVO for fracture detection: Analytic basis and practical solutions” TLE, Vol.16, No. 10, 1429–1434.

Rutherford S.R. & Williams R.H., 1989 “Amplitude-versus-offset variations in gas sands” Geophysics 54, 680-688

Shuey R.T, 1985 “A simplification of the Zoeppritz equations” Geophysics 50, 609-615.

Wang Y,1999 “Approximation of the Zoeppritz equations and their use in AVO analysis” Geophysics, 641920-1937

Williams M., Jenner E., “Interpreting seismic data in the presence of azimuthal anisotropy: or azimuthal anisotropy in the presence of the seismic interpretation” TLE Vol. 21, No. 8, pp. 771-774.